THE JOURNAL OF PHYSICAL CHEMISTRY C

ARTICLE

pubs.acs.org/JPCC

Synthesis, Photoluminescence, and Magnetic Properties of Nitrogen-Doping Helical Carbon Nanotubes

Jianfeng Wen,[†] Yang Zhang,[†] Nujiang Tang,[*,†] Xiangang Wan,[†] Zhuhong Xiong,[‡] Wei Zhong,[†] Zhenlin Wang,[†] Xinglong Wu,[†] and Youwei Du[†]

[†]Nanjing National Laboratory of Microstructures, Nanjing University, Nanjing 210093, People's Republic of China

[‡]School of Physics Science & Technology, Southwest University, Chongqing 400715, People's Republic of China

ABSTRACT: Over Ni nanoparticles generated by means of a combined sol−gel/reduction method, helical carbon nanotubes (HCNTs) were synthesized in acetylene pyrolysis at 425 °C. By annealing the pristine HCNTs in NH_3 atmosphere, the N-doped HCNTs were obtained. The dependence of annealing temperature on the nitrogen content and doping type of the N-doped HCNTs was studied. The photoluminescence (PL) properties of the pristine HCNTs and N-doped HCNTs were examined systematically at room temperature (RT). The results demonstrated that the pristine HCNTs exhibit strong ultraviolet (UV) PL at 368 nm. By doping the pyridinic and graphitic N into the pristine HCNTs, the UV PL could be enhanced. Moreover, the magnetic properties of the pristine and N-doped HCNTs have been measured.

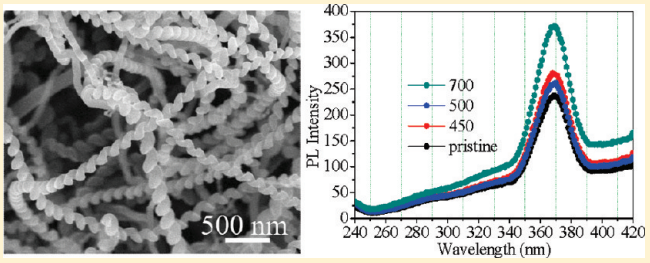

INTRODUCTION

Helical carbon nanotubes (HCNTs), with their outstanding physical and chemical properties and potential applications,[1,2] have aroused special attention since they were observed by Amelinckx et al.[3] in 1994. It is found that HCNTs exhibit unique electrical and mechanical properties that could be utilized in nanoengineering.[4−8] It is well know that in addition to the outstanding physical and chemical properties, the CNTs also possess novel linear and nonlinear optical properties, and their electronic properties are strongly dependent on the size, structure, and impurity.[9] However, as to HCNTs, nearly all experimental work has focused on their electrical, mechanical, and microwave absorption properties. Little work has been done on the optical properties.

Moreover, UV-light-emitting materials have aroused continual and tremendous interest because the light in the UV region has extensive applications, such as photolithography, optical data storage, and medical analysis and treatment.[10,11] Recently, UV PL was found at 385 nm (3.22 eV) from ZnO nanowire arrays,[12] at 333 nm (3.72 eV) from wurtzite ZnS nanowires,[13] and at 357 nm (3.47 eV) from GaN.[14] However, despite the tremendous amount of effort that has been devoted, UV-light-emitting materials are still rare. Therefore, to find other new UV-light-emitting materials is of both fundamental and technological importance. Thus, studying their PL properties is an interesting problem, which we address in the present work.

Notable, many efforts have been devoted to study one-dimensional N-doped carbon materials because doping nitrogen into carbon materials could be a promising way to improve their electronic, mechanical, and optical properties for various applications.[15−17] Compared to C and CNx nanotube diodes, the C/CNx multiwalled nanotube diode exhibits a large photocurrent and a large photovoltage under illumination, showing a clear rectification effect.[18] A large photocurrent can be produced because of the influence of the strong electric field in the vicinity of the C/CNx junction. Both experimental and theoretical investigations demonstrate that N-doped CNTs show enhanced field emission properties compared to pure CNTs[19,20] and cause a shift in the dominant emission to lower energies.[21] Hagiri et al.[22] have theoretically studied the heteroatom-substituted π-conjugated systems and have confirmed that the different heteroatom arrangements cause the different spin-stable states of the singlet and the triplet and that replaced N atom as a spin cap induces the π electron excess.

Up to now, N-doped one-dimensional carbon materials, including carbon nanofibers[23,24] and CNTs,[25−30] have been successfully synthesized and well studied. However, there are few reports on the large-scale synthesis of N-doped HCNTs. We have successfully synthesized HCNTs with high yield via the low-temperature catalytic chemical vapor decomposition (CCVD) route and have systematically investigated their growth dependence on catalytic particle size, single nanohelix electrical properties, and magnetic and microwave absorption properties.[31−34] Herein, we report on a systematic investigation into the PL properties of the pristine HCNTs at room temperature (RT). Under optical excitation, the pristine HCNTs exhibit strong UV PL at 368 nm at RT. Interestingly, by doping the pyridinic and graphitic N into the pristine HCNTs, the UV PL could be

Received: March 23, 2011
Revised: May 12, 2011
Published: May 23, 2011

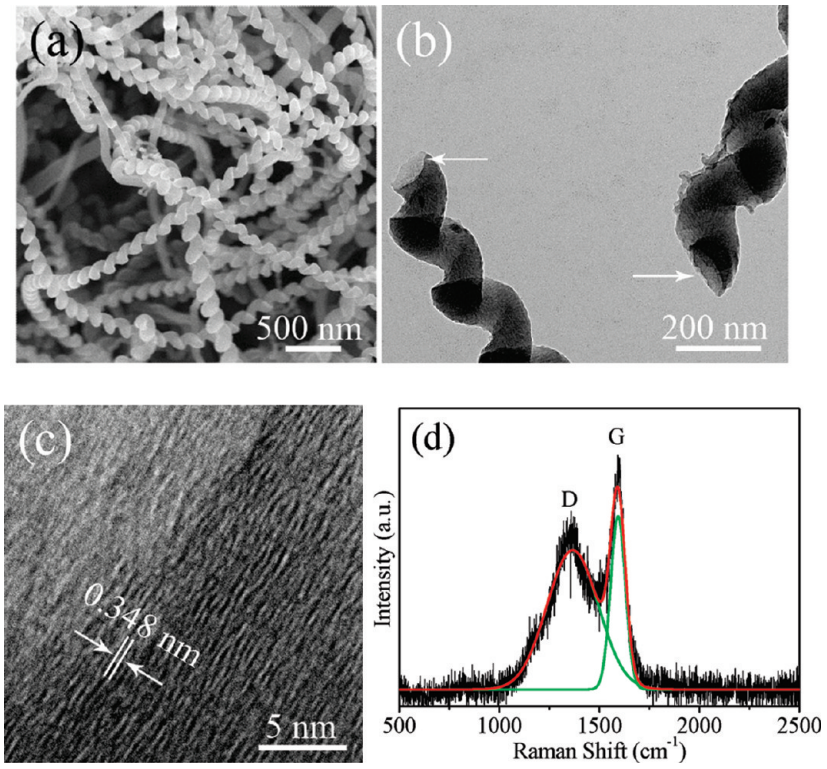

Figure 1. Microstructure of the pristine HCNTs: (a) FESEM image; (b) a typical TEM image of the pristine HCNT after being ultrasonically dispersed in distilled water for 9 h; the white arrows indicate the nozzles of the HCNTs; (c) HRTEM image; and (d) Raman spectrum. The black lines, red lines, and green lines are measured curves, fitting curves, and fitted single peaks, respectively.

enhanced. The N-doped HCNTs with high nitrogen content were synthesized via annealing the pristine HCNTs in an NH_3 atmosphere. The dependences of annealing temperature on the magnetic properties, nitrogen content, and doping type of the N-doped HCNTs were also studied.

EXPERIMENTAL SECTION

For the synthesis of pristine HCNTS, the preparation of catalyst precursors is similar to our previous work.[31−34] Namely, 0.01 mol $Ni(NO_3)_2 \cdot 6H_2O$ and 0.03 mol citric acid monohydrate were dissolved in 100 mL of absolute ethanol and stirred at 60 °C for 4 h. Then, the ethanol was evaporated at 88 °C, and the residue was heated in air at 350 °C for 4 h. The growth of high-purity HCNTs employs the CCVD method. In brief, 0.025 g of nickel oxide powder was spread evenly on a ceramic plate and placed inside of a quartz reaction tube (4.94 cm in inner diameter and 68.3 cm in length, equipped with temperature and gas-flow controls). After the nickel oxide was reduced in H_2 at 365 °C for 1 h, the temperature was raised to 425 °C, and C_2H_2 gas was introduced into the reaction tube over the reduced nickel nanoparticles with the flow of 15 sccm for 1 h at atmospheric pressure. After the furnace cooled to RT, ∼1.863 g of sample could be obtained.

For the synthesis of N-doped HCNTS, the doping of nitrogen was performed by annealing pristine HCNTs in an NH_3 atmosphere using the same annealing system as that above. Some of the pristine HCNTs were put in a ceramic crucible and placed inside of the quartz tube and then were annealed at appropriate temperatures for 4 h in an NH_3 atmosphere. After the furnace cooled to RT, the N-doped sample was obtained.

The morphologies of the samples were examined by TEM (Model JEOL-2010, Japan) operated at an accelerating voltages of 120 kV and by FESEM (Model JSM-6700F, JEOL, Japan) at an accelerating voltage of 5 kV. The nitrogen content in N-doped HCNTs was determined by XPS (Thermo Fisher Scientific, K-Alpha). The Raman spectrum was obtained by an InVia Raman system (Renishaw, England) using a 514.5 nm laser as the light source. The PL spectra were obtained at ambient conditions by a spectrofluorophotometer (Shimadzu RF-5301PC) using a Xe lamp as the light source. For PL spectra investigation, ∼1.0 mg of powdered samples were ultrasonically dispersed in 9 mL of distilled water for 9 h and kept in quiescence for about 4 h. After that, the supernatant was used. The magnetic properties of the samples were measured at RT by a Quantum Design MPMS SQUID magnetometer (Quantum Design MPMS-XL, USA) equipped with a superconducting magnet capable of producing fields of up to 65 kOe.

RESULTS AND DISCUSSION

Microstructures and PL Properties of Pristine HCNTs. The morphology of the pristine HCNTs was first characterized using FESEM. Shown in Figure 1a is the FESEM image of the pristine HCNTs. One can find that most of the products have a helical structure; only a few of them show a straight-like form. Namely, the pristine sample has a high-purity helical structure. From Figure 1a, one can estimate the diameter of the HCNTs, which is in the range of 80−160 nm. We have destroyed the HCNTs via ultrasonically dispersing them in distilled water for 9 h, and the TEM image shows the clear hollow core (as indicated by white arrows shown in Figure 1b). It demonstrates that our carbon

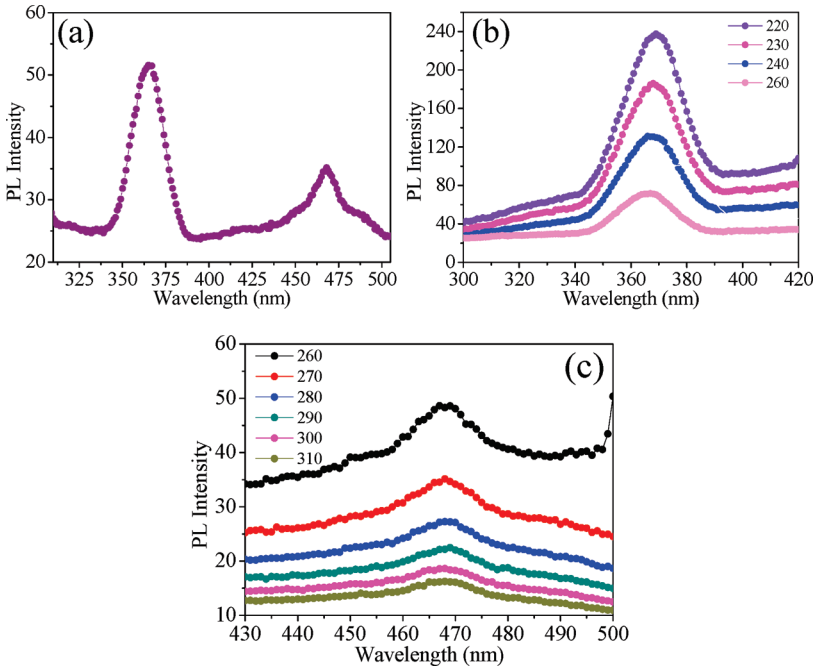

Figure 2. PL spectra of the pristine HCNTs: (a) with excitation wavelength 270 nm; (b) with different excitation wavelengths from 220 to 260 nm; and (c) with different excitation wavelengths from 260 to 310 nm.

products are not coiled carbon nanowires but HCNTs. Note that the hollow part of the HCNT cannot be observed clearly, which may attribute to the very thin walls, as corroborated by the TEM image in Figure 4c. Namely, it demonstrates further that our carbon products are not coiled carbon nanowires but HCNTs.

Our previous works show that these helical carbon materials have a graphitic structure with lots of defects.[31−34] Shown in Figure 1c is the HRTEM image of the pristine HCNTs. It reveals that the graphite layers are distorted and disordered. Namely, there are a lot of defects in the pristine HCNTs. Moreover, one can find that the interlayer spacing is ∼0.348 nm. We determined the Raman shift of the pristine HCNTs, and the spectrum is shown in Figure 1d. Similar to our previous work on pristine HCNTs,[31−34] there are two bands in the Raman spectrum, one peak called the G band at ∼1595 cm^{-1}, which is known to originate from graphitic sp^2-bonded carbon, and the other D band at 1334 cm^{-1}, which originated from the disorder carbons. The Raman spectrum was fitted and deconvoluted. The intensity ratio of the D and G bands I_D/I_G is 0.8, indicating the high ratio of defects in the pristine HCNTs. Notably, our FESEM and Raman investigation (as shown in Figure 3c) provides little indication of any change in morphology and structure after annealing the pristine HCNTs in an NH_3 atmosphere.

To explore the optical properties of as-prepared pristine HCNTs, a detailed PL study was carried out at RT by using different excitation wavelengths. Shown in Figure 2a is the PL spectra of the pristine HCNTs with an excitation wavelength of 270 nm. The PL intensity is so high that the emission spots can be easily observed. It is interesting to see that there is a clear strong peak centered at 368 nm and a sideband peak centered at 468 nm. Namely, one of the peaks is in the UV range, and the other is in the blue range. Moreover, the PL intensity of the peak centered at 368 nm is much stronger than that of the peak centered at 468 nm. Apparently, it is different from other carbon nanostructures such as CNTs, carbon nanoparticles, and graphene quantum dots (GQDs) that there is only one peak in the blue range PL.[35−37] Figure 2b and c shows the PL spectra of N-doped HCNTs with different excitation wavelengths from 220 to 260 nm and 260 to 310 nm, respectively. As shown in Figure 2b, under optical excitation, the pristine HCNTs exhibit strong UV PL at 368 nm along with strong and broad 350−390 nm UV PL at RT. With the excitation wavelength increasing from 220 to 260 nm, one can find that the intensity of the PL peak centered at 368 nm decreases rapidly, and the intensity of the PL peak reaches a maximum at an excitation wavelength of 220 nm. However, the peak position almost keeps relatively stable, namely, no apparent blue shift or red shift in the peak can be observed. It is the same for the case of the peak centered at 468 nm (shown in Figure 2c). Interestingly, this excitation-dependent PL behavior is different from the red shift of GQDs and most carbon nanoparticles.[35−37] Notably, the results show that the energy of the luminescence peak is higher than that of ZnO nanowire arrays at 3.22 eV (385 nm)[12] and comparable to that observed from gallium nitride (GaN) at 3.47 eV (357 nm).[14]

Microstructures and PL Properties of N-Doped HCNTs. Many researches confirmed that the doping of N atoms into carbon materials can improve their field emission properties[19,20] and favor PL emission,[38] and the electronic properties of carbon-based materials can effectively be tuned via doping N, which is determined by the doping type, doping content, and so forth. Generally, there are two routes to dope nitrogen into carbon materials, directly doping during the synthesis process or doping by post-treatment. For the latter, carbon materials are often treated in a nitrogen-containing atmosphere. For example, Jiang et al.[39] annealed the pristine CNTs in flowing NH_3 at 600 °C for 3 h and found that the products generate nitrogen-containing groups, and we have annealed the pristine HCNTs in NH_3 for 4 h at 450, 500, and 700 °C, respectively. To detect the nitrogen content and the bonding environment of the C and N species of the N-doped HCNTs, XPS was employed. The N contents

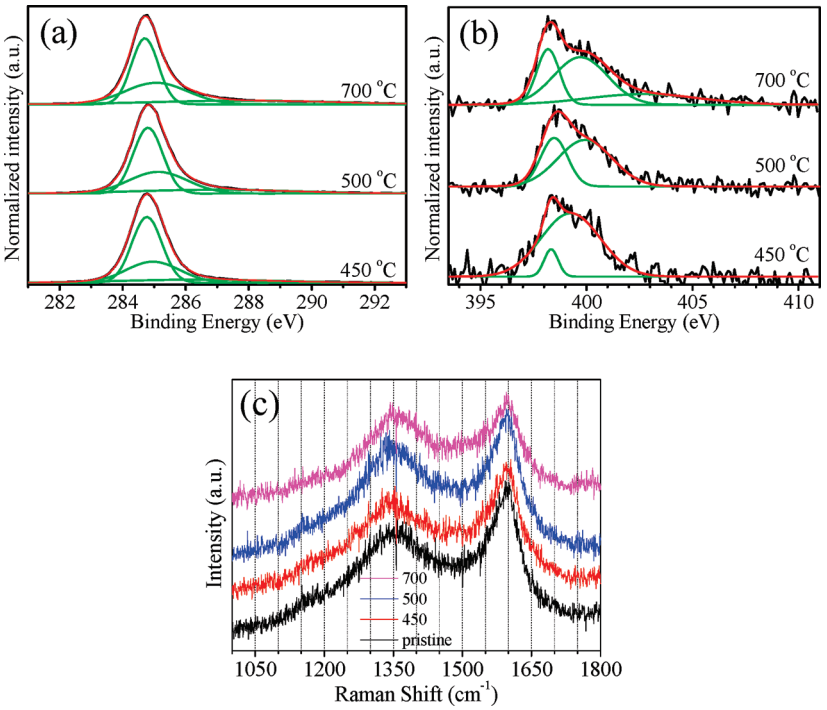

Figure 3. Normalized XPS spectra of the N-doped HCNTs obtained at different annealing temperatures: (a) fine-scanned C 1s spectra and (b) fine-scanned N 1s spectra. The black lines, red lines, and green lines are measured curves, fitting curves, and fitted single peaks, respectively. (c) Raman spectra.

defined as 100N/(C + N) atom % of the samples annealed at 450, 500, and 700 °C are 1.8, 5.3, and 4.6 atom %, respectively. In order to get information on the incorporation of nitrogen into carbon, the C 1s and N 1s spectra were fine-scanned (shown in Figure 3a and b). Shown in Figure 3a are the C 1s spectrum and its fitted curve. The C 1s peak was deconvoluted into three bands at 284.8, 285.1, and 287.1 eV. The strongest peak centered at 284.8 eV is assigned to C−C bond. It is in agreement with previously reported values for N-doped CNTs.[40] The weak peak centered at 285.1 eV belongs to the C−N bond.[29] It confirmed that N atoms have been successfully doped into HCNTs and bonded to C atoms. The weakest band at 287.1 eV can be ascribed to the C═O or C−N bond.[41] To get more information on the doping type at various temperatures, the N 1s spectra of the samples annealed at different temperature were fine-scanned and deconvoluted into two bands at 398.5 and 400.1 eV, which can be assigned to pyridinic (398.5 eV) and pyrrolic (400.1 eV) N types, respectively (shown in Figure 3b).[42−44] As shown in Figure 3b, when the annealing temperatures are 450 and 500 °C, there are two bands at ∼398.5 and 400.1 eV in the two samples, which correspond to pyridinic and pyrrolic N, respectively. Furthermore, the third component of 402.9 eV appeared in the sample annealed at 700 °C. This broad component that appeared at high binding energy can be assigned to the graphitic N (i.e., N atoms replacing C atoms on the graphitic layers).[42] The results demonstrate that the pyrrolic N and the pyridinic N are the main doping types in the two samples annealed at 450 and 500 °C. In other words, at relatively low annealing temperatures of 450 and 500 °C, the N atoms bond to C just on the edge or defect of the HCNTs in an NH_3 atmosphere. However, N atoms could substitute inner C atoms in the graphitic layers of the HCNTs at high temperatures of 700 °C. Namely, it demonstrates further that N atoms have been successfully bonded to carbon atoms, and we have successfully synthesized N-doped HCNTs by annealing the pristine HCNTs in an NH_3 atmosphere.

Figure 4a shows the PL spectra of the pristine and the N-doped samples obtained at different annealing temperatures, and the excitation wavelength is 270 nm. It is similar to the case of the pristine HCNTs; there are two PL bands in all of the N-doped samples; one is strong in the UV range (at ∼368 nm), and the other is relatively weak in the blue range (at ∼468 nm). Interestingly, one can find that (i) the N-doped HCNTs showed a clear enhancement in the intensity of both peaks compared to the pristine HCNTs; (ii) the enhancement in the samples annealed at 450 and 700 °C is more apparent than that of the sample annealed at 500 °C; that (iii) there is no clear shift in the peak position in the pristine and all of the N-doped samples. It is well know that both the structure and defect affect the electronic structure and magnetic properties of the nanosystem, consequently changing their optical feature significantly.[9] Therefore, it is reasonable to conclude that (i) pyridinic and graphitic N can enhance the PL and (ii) with the increasing annealing temperature, the graphitic N content increases, and as a result, the PL can be enhanced greatly. That is, the incorporation of nitrogen has changed the electronic structure of the HCNTs, resulting in the change of PL. Apparently, one can obtain strong room-temperature UV PL in N-doped HCNTs with high graphitic N content by annealing pristine HCNTs at high temperature. Figure 4c is a typical TEM image of the N-doped HCNT annealed at 700 °C in NH_3 atmosphere after being ultrasonically dispersed in acetone for 2 min, and the white arrows indicate the rupture parts of the N-doped HCNT. This confirms further that our carbon products are not coiled carbon nanowires but HCNTs, and the walls of both the HCNT and N-doped HCNT are very thin.

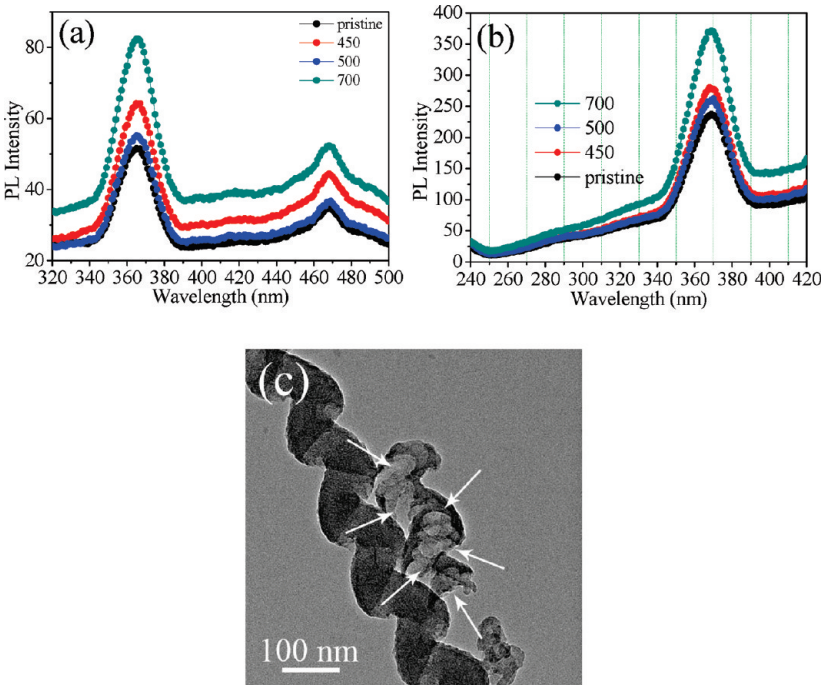

Figure 4. PL spectra of the pristine and N-doped HCNTs obtained at different annealing temperatures: (a) with the excitation wavelength of 270 nm and (b) with the excitation wavelength of 220 nm. (c) A typical TEM image of the N-doped HCNT annealed at 700 °C in an NH_3 atmosphere after being ultrasonically dispersed in acetone for 2 min; the white arrows indicate the destroyed parts of the N-doped HCNT.

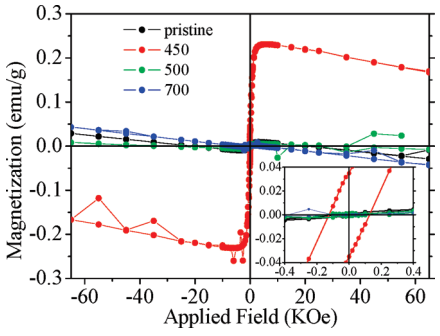

Figure 5. Typical magnetization curves of the pristine and N-doped HCNTs samples obtained at different annealing temperatures measured at 300 K by SQUID. The inset is a part of the magnetization curves.

Magnetic Properties of the Pristine and N-Doped HCNTs. Figure 5 shows the M-H curves of the pristine and N-doped HCNTs sample measured at 300 K. One can find that the magnetization of all of the samples is both ferromagnetic and diamagnetic. The ferromagnetism of the sample mainly originates from the Ni nanoparticles, and the diamagnetism mainly originates from N-doped HCNTs. The saturation magnetization (M_S) and the coercivity (H_c) of the sample annealed at 450 °C were 0.231 emu/g and 124.85 Oe, respectively. However, the pristine sample and the samples annealed at 500 and 700 °C have low magnetization. This phenomenon can be attributed to the oxidation, carbonization, or nitrogenization of the nickel nanoparticles. For our experiment, the nickel oxide was reduced by H_2 and used as a catalyst to prepare HCNTs. Thus, the nickel nanoparticles should be partly carbonized or nitrogenized and form the compounds of Ni_3C[45] or Ni−N alloys[46] (eg., NiN, Ni_3N, Ni_4N, Ni_8N, etc.). Note that Ni_3C decomposes to Ni and C above 430 °C.[47] In other words, almost no Ni_3C should exist above 450 °C. Namely, above 450 °C, the nickel nanoparticles should be only partly nitrogenized and form the Ni−N alloys. As we know Ni_3C[48,49] and most of Ni−N alloys[50,51] are nonmagnetic, and the M_S of them are near 0. Therefore, the M_S of the pristine sample and that of the samples annealed at 500 and 700 °C obtained experimentally are very low, which can be attributed to the low content of metallic Ni. By contrast, the M_S of the sample annealed at 450 °C is relatively high maybe because of the relatively high content of Ni. Namely, a relatively high magnetization value is observed for the N-doped HCNTs annealed at 450 °C due to the encapsulation of Ni nanoparticles at the nodes between the nanotubes. In other words, in the as-prepared sample and the samples annealed at 500 and 700 °C, Ni_3C or Ni−N alloys are the predominant Ni phase, whereas in the sample annealed at 450 °C, Ni is the abundant Ni phase. In other words, the annealing process can be used to change the relative proportions of Ni and Ni_3C and Ni−N alloys in the samples.

CONCLUSIONS

In conclusion, we have successfully synthesized N-doped HCNTs by annealing the pristine HCNTs in an NH_3 atmosphere. The study showed that HCNTs can have UV PL at 368 nm. By doping of pyridinic and graphitic N into the pristine HCNTs, the PL can be enhanced. Furthermore, we have illustrated how the nitrogen content, doping type, and optical property of the N-doped HCNTs can be manipulated. By selecting an annealing temperature, one can tailor PL via tuning of the nitrogen content and the doping type of the N-doped HCNTs. Relatively high magnetization was observed over the N-doped HCNTs annealed at 450 °C due to the encapsulation of a Ni nanoparticle at the node.

AUTHOR INFORMATION

Corresponding Author
*E-mail: tangnujiang@nju.edu.cn.

ACKNOWLEDGMENT

This work was financially supported by the NSFC (Grant No. 51072079, 10734010) and State Key Program for Basic Research (Grant No. 2010CB923402 and 2007CB613204), People's Republic of China.

REFERENCES

(1) Ouyang, Z. C.; Su, Z. B.; Wang, C. L. *Phys. Rev. Lett.* **1997**, *78*, 4055.
(2) Bajpai, V.; Dai, L. M.; Ohashi, T. *J. Am. Chem. Soc.* **2004**, *126*, 5070.
(3) Amelinckx, S.; Zhang, X. B.; Bernaerts, D.; Zhang, X. F.; Ivanov, V.; Nagy, J. B. *Science* **1994**, *265*, 635.
(4) Akagi, K.; Tamura, R.; Tsukada, M.; Itoh, S.; Ihara, S. *Phys. Rev. Lett.* **1995**, *74*, 2307.
(5) Volodin, A.; Ahlskog, M.; Seynaeve, E.; Haesendonck, C. Van; Fonseca, A.; Nagy, J. B. *Phys. Rev. Lett.* **2000**, *84*, 3342.
(6) Fonseca, A. F. Da; D. Galvao, S. *Phys. Rev. Lett.* **2004**, *92*, 175502.
(7) Chen, X. Q.; Zhang, S. L.; Dikin, D. A.; Ding, W. Q.; Ruoff, R. S.; Pan, L. J.; Nakayama, Y. *Nano Lett.* **2003**, *3*, 1299.
(8) Volodin, A.; Buntinx, D.; Ahlskog, M.; Fonseca, A.; Nagy, J. B.; Haesendonck, C. Van. *Nano Lett.* **2004**, *4*, 1775.
(9) Wan, X. G.; Dong, J. M.; Xing, D. Y. *Phys. Rev. B* **1998**, *58*, 6756.
(10) Oto, T.; Banal, R. G.; Kataoka, K.; Funato, M.; Kawakami, Y. *Nat. Photonics* **2010**, *4*, 767.
(11) Li, L. H.; Chen, Y.; Lin, M. Y.; Glushenkov, A. M.; Cheng, B. M.; Yu, J. *Appl. Phys. Lett.* **2010**, *97*, 141104.
(12) Huang, M. H.; Mao, S.; Feick, H.; Yan, H. Q.; Wu, Y. Y.; Kind, H.; Weber, E.; Russo, R.; Yang, P. D. *Science* **2001**, *292*, 1897.
(13) Chen, R.; Li, D. H.; Liu, B.; Peng, Z. P.; Gurzadyan, G. G.; Xiong, Q. H.; Sun, H. D. *Nano Lett.* **2010**, *10*, 4956.
(14) Schmidt, T. J.; Cho, Y. H.; Song, J. J.; Yang, W. *Appl. Phys. Lett.* **1999**, *74*, 245.
(15) Yang, Q. H.; Hou, P. X.; Unno, M.; Yamauchi, S.; Saito, R.; Kyotani, T. *Nano Lett.* **2005**, *5*, 2465.
(16) Xiao, K.; Fu, Y.; Liu, Y. Q.; Yu, G.; Zhai, J.; Jiang, L.; Hu, W. P.; Shuai, Z. G.; Luo, Y.; Zhu, D. B. *Adv. Funct. Mater.* **2007**, *17*, 2842.
(17) Nevidomskyy, A. H.; Csanyi, G.; Payne, M. C. *Phys. Rev. Lett.* **2003**, *91*, 105502.
(18) Ganesan, Y.; Peng, C.; Lu, Y.; Ci, L. J.; Srivastava, A.; Ajayan, P. M.; Lou, J. *ACS Nano* **2010**, *4*, 7637.
(19) Wang, X. B.; Liu, Y. Q.; Zhu, D. B.; Zhang, L.; Ma, H. Z.; Yao, N.; Zhang, B. L. *J. Phys. Chem. B* **2002**, *106*, 2186.
(20) Wang, C.; Qiao, L.; Qu, C. Q.; Zheng, W. T.; Jiang, Q. *J. Phys. Chem. C* **2009**, *113*, 812.
(21) Li, L. J.; Glerup, M.; Khlobystov, A. N.; Wiltshire, J. G.; Sauvajol, J. L.; Taylor, R. A.; Nicholas, R. J. *Carbon* **2006**, *44*, 2752.
(22) Hagiri, I.; Takahashi, N.; Takeda, K. *J. Phys. Chem. A* **2004**, *108*, 2290.
(23) Terrones, M.; Redlich, P.; Grobert, N.; Trasobares, S.; Hsu, W. K.; Terrones, H.; Zhu, Y. Q.; Hare, J. P.; Reeves, C. L.; Cheetham, A. K.; Ruhle, M.; Kroto, H. W.; Walton, D. R. M. *Adv. Mater.* **1999**, *11*, 655.
(24) Terrones, M.; Terrones, H.; Grobert, N.; Hsu, W. K.; Zhu, Y. Q.; Hare, J. P.; Kroto, H. W.; Walton, D. R. M.; Kohler-Redlich, P.; Ruhle, M.; Zhang, J. P.; Cheetham, A. K. *Appl. Phys. Lett.* **1999**, *75*, 3932.
(25) Chen, H.; Yang, Y.; Hu, Z.; Huo, K. F.; Ma, Y. W.; Chen, Y.; Wang, X. S.; Lu, Y. N. *J. Phys. Chem. B* **2006**, *110*, 16422.
(26) Glerup, M.; Castignolles, M.; Holzinger, M.; Hug, G.; Loiseau, A.; Bernier, P. *Chem. Commun.* **2003**, *20*, 2542.
(27) Xu, W. H.; Kyotani, T.; Pradhan, B. K.; Nakajima, T.; Tomita, A. *Adv. Mater.* **2003**, *15*, 1087.
(28) Kim, S. Y.; Lee, J.; Na, C. W.; Park, J.; Seo, K.; Kim, B. *Chem. Phys. Lett.* **2005**, *413*, 300.
(29) Ayala, P.; Grueneis, A.; Gemming, T.; Grimm, D.; Kramberger, C.; Ruemmeli, M. H.; Freire, F. L.; Kuzmany, H.; Pfeiffer, R.; Barreiro, A.; Buechner, B.; Pichler, T. *J. Phys. Chem. C* **2007**, *111*, 2879.
(30) Lin, H.; Arenal, R.; Enouz-Vedrenne, S.; Stephan, O.; Loiseau, A. *J. Phys. Chem. C* **2009**, *113*, 9509.
(31) Tang, N. J.; Zhong, W.; Gedanken, A.; Du, Y. W. *J. Phys. Chem. B* **2006**, *110*, 11772.
(32) Tang, N. J.; Zhong, W.; Au, C. T.; Gedanken, A.; Yang, Y.; Du, Y. W. *Adv. Funct. Mater.* **2007**, *17*, 1542.
(33) Tang, N. J.; Wen, J. F.; Zhang, Y.; Liu, F. X.; Lin, K. J.; Du, Y. W. *ACS Nano* **2010**, *4*, 241.
(34) Tang, N. J.; Kuo, W.; Jeng, C. C.; Wang, L. Y.; Lin, K. J.; Du, Y. W. *ACS Nano* **2010**, *4*, 781.
(35) Pan, D. Y.; Zhang, J. C.; Li, Z.; Wu, M. H. *Adv. Mater.* **2010**, *22*, 734.
(36) Pan, D. Y.; Zhang, J. C.; Li, Z.; Wu, C.; Yan, X. M.; Wu, M. H. *Chem. Commun.* **2010**, *46*, 3681.
(37) Zhang, J. C.; Shen, W. Q.; Pan, D. Y.; Zhang, Z. W.; Fang, Y. G.; Wu, M. H. *New J. Chem.* **2010**, *34*, 591.
(38) Papadimitriou, D.; Roupakas, G.; Dimitriadis, C. A.; Logothetidis, S. *J. Appl. Phys.* **2002**, *92*, 870.
(39) Jiang, L. Q.; Gao, L. *Carbon* **2003**, *41*, 2923.
(40) Maldonado, S.; Morin, S.; Stevenson, K. J. *Carbon* **2006**, *44*, 1429.
(41) Wang, Y.; Shao, Y. Y.; Matson, D. W.; Li, J. H.; Lin, Y. H. *ACS Nano* **2010**, *4*, 1790.
(42) Casanovas, J.; Ricart, J. M.; Rubio, J.; Illas, F.; Jimenez-Mateos, J. M. *J. Am. Chem. Soc.* **1996**, *118*, 8071.
(43) Panchakarla, L. S.; Govindaraj, A.; Rao, C. N. R. *ACS Nano* **2007**, *1*, 494.
(44) Panchakarla, L. S.; Govindaraj, A.; Rao, C. N. R. *Inorg. Chim. Acta* **2010**, *363*, 4163.
(45) Bonder, M. J.; Kirkpatrick, E. M.; Martin, T.; Kim, S. J.; Rieke, R. D.; Leslie-Pelecky, D. L. *J. Magn. Magn. Mater.* **2000**, *222*, 70.
(46) Neklyudov, I. M.; Morozov, A. N. *Physica B* **2004**, *350*, 325.
(47) Nagakura, S. *J. Phys. Soc. Jpn.* **1957**, *12*, 482.
(48) Yue, L. P.; Sabiryanov, R.; Kirkpatrick, E. M.; Leslie-Pelecky, D. L. *Phys. Rev. B* **2000**, *62*, 8969.
(49) Shein, I. R.; Medvedeva, N. I.; Ivanovskii, A. L. *Physica B* **2006**, *371*, 126.
(50) Vempaire, D.; Fettar, F.; Ortega, L.; Pierre, F.; Miraglia, S.; Sulpice, A.; Pelletier, J.; Hlil, E. K.; Fruchart, D. *J. Appl. Phys.* **2009**, *106*, 073911.
(51) Wang, H. B.; Xue, D. S. *Chin. Phys. Lett.* **2004**, *21*, 1612.